

A review of experimental and numerical analysis on laser beam machining of composites and thermoplastics

Kaveh Moghadasi¹, Khairul Fikri Tamrin^{1*}, Fahizan Mahmud², Marzie Hatf Jalil³

¹Department of Mechanical and Manufacturing Engineering, Faculty of Engineering, Universiti Malaysia Sarawak (UNIMAS), 94300 Kota Samarahan, Sarawak, Malaysia

²Murata Manufacturing (Sarawak) Sdn. Bhd.

³Department of Design Technology, Faculty of Applied and Creative Arts, Universiti Malaysia Sarawak (UNIMAS), 94300 Kota Samarahan, Sarawak, Malaysia

*Corresponding author: Email: tkfikri@unimas.my (K.F.Tamrin) | Tel: +601115653090 | Fax: +6082583410

Received: 03-07-2022, Received in Revised form: 08-03-2023, Accepted: 20-03-2023, Published: 20-03-2023

Abstract

Material cutting is a crucial process owing to its strategic value in producing items such as aircraft, ships, automobiles, biomedical components, etc. Laser beam cutting is among the efficient techniques for creating complicated geometries with rigorous design criteria. This article discusses the experimental study of the laser -cutting process and the effect of laser -cutting parameters on composites and thermoplastics. Several numerical modeling and different optimization approaches employed by various researchers are also reviewed in this article.

Keywords: Laser, composite, polymer, cut characteristics, numerical modeling.

Introduction

With growing production rates of structures/components required in the aerospace, marine, chemical processing equipment, sporting goods, automobiles and military sectors, there is a necessary demand for time- and cost-efficient manufacturing processes for rapid and volume production [1, 2]. Conventional contact methods of cutting materials e.g., milling machine, sawing or drilling, result in high tool wear, poor cut surface quality and delamination [3, 4].

Numerous non-conventional machining techniques are employed in the industry, for instance laser beam machining (LBM), electro discharge machining (EDM), ion beam machining (IBM), jet machining (JM), and Ultrasonic machining (UM) processes [5-9]. To manufacture complex and accurate shapes of different materials such as titanium, ceramics, fiber-reinforced composites, and thermoplastics, aforementioned techniques are used to facilitate the machining process compared to conventional processing methods. However, limitations of non-conventional methods also exist in terms of geometry accuracy and complexity, type of materials, etc. [10]. Therefore, it is necessary for operators to select appropriate process with several criteria for a particular application. Among these non-conventional machining technologies, LBM has become a specialty machining technology and has greatly attracted attention due to its capability in the machining of a broad range of materials with high precision [11, 12]. According to [13], the term “laser” is an abbreviation for light amplification by stimulated emission of radiation. The idea of using light for machining has attracted humankind’s attention since the first time they discovered the method of burning paper on a sunny day with the aid of a magnifying glass. Common types of lasers currently used in industries are CO₂, excimer, Nd:YAG and fiber lasers.

Laser has become an essential tool for material removal in typical applications such as drilling, cutting, scribing, marking, ablation and welding/joining. Material removal in LBM usually consists of three stages: a) melting, b) vaporization, and c) degradation of mechanical strength and chemical deterioration due to the breaking of chemical bonds [14]. The properties of the workpiece are also influential in successful material removal especially latent heat of vaporization, thermal diffusivity, thermal conductivity and surface reflectivity. Laser cutting has been widely employed in process industries in many countries because it is an effective way to perform precise

cutting due to its non-contact method [15, 16]. Laser cutting has better advantages in terms of surface finishing, cut quality and fast cutting when compared to other competing processes. Additionally, it decreases the manufacturing cost because it can be integrated into assembly lines and programmed using computers to fabricate complex geometrical cuts. This article reviews the experimental and numerical laser cutting process of composites and polymers reported in the literature. Moreover, the effects of selected laser parameters on cut characteristics are discussed.

1. Classification of Materials

1.1 Composites

Composites combine two or more constituent materials with significantly different mechanical, thermal and chemical properties to form a new material type with outstanding functional characteristics. The most popular synthetic composites are carbon fiber -reinforced polymer (CFRP), glass fiber -reinforced polymer (GFRP), and Kevlar fiber -reinforced polymer (KFRP). In recent years, synthetic fiber -reinforced polymers in high-performance structural applications have increased dramatically due to developments in processing technology, enabling products/parts with excellent strength-to-weight ratio production. For instance, GFRP composites are found in fairings, storage room doors, landing gear doors and passenger compartments. CFRP composites are often used in wing boxes, horizontal stabilizers, vertical stabilizers and wing panels [17, 18]. In addition to CFRP and GFRP, KFRP composites are also used for many aerospace, military and automotive applications [19]. Natural fiber has recently been considered a renewable source and a new generation of reinforcement for polymer -based materials. Natural fibers are a prominent material often adopted to replace synthetic materials in applications where reduced weight and energy conservation are crucial [20-22]. Cotton fiber laminate (CFL), a type of natural fiber composite, is very useful for electrical insulation applications at low voltages. The shapes of CFL may come in many geometrical forms and are usually found in gears, spacers and coil support in turbine generators. Ceramic matrix composites (CMCs) consist of glass-ceramics, silicon carbide and carbon. These composites represent a new class of integrally woven ceramic-matrix-composites for high-temperature applications, where strength and thermal conductivity are essential. Their mechanical properties include high strength and stiffness at very high temperatures, low



density, high damage tolerance and thermal shock resistance [23]. Metal matrix composites (MMCs), owing to their unique physical/mechanical properties, and performance, have been considered for applications in the automotive and aerospace industries. MMCs possess superior properties at elevated temperatures, high thermal conductivity, high strength and stiffness, high strength-to-density ratio and low coefficient of thermal expansion [24].

1.2 Polymers

Due to their versatility and adaptable chemical and physical qualities, thermoplastic polymers are extensively utilized as substrates in automotive, electronic components, and portable device packaging applications [25]. When subjected to re-heating and re-moulding procedures, thermoplastics would demonstrate superior fatigue resistance and fracture toughness as compared to thermoset and elastomer. Polycarbonate (PC), polypropylene (PP), and polymethyl methacrylate (PMMA) are thermoplastics that are widely recognised. Among the numerous applications of these thermoplastics is the use of PC as optical lenses and safety eyewear. As a result of its low cost and mouldability, PP has been increasingly employed in the biology and medical disciplines, for example, in the production of polymerase chain reaction (PCR) tubes and tips for biochemical experimentation and medication storage. PMMA, on the other hand, provides superior environmental stability as a lightweight and nonporous solid [26]. It is used for various functions, including window glazing, lens meter covers, etc., at relatively inexpensive costs.

2. Quality Characteristics of Laser Cutting

In the laser cutting process, the material substrate is quickly heated by laser radiation, which increases the temperature of the surrounding region through conduction before significant

melting occurs, as illustrated in **Figure 1a**. By providing a relative motion between the laser beam and the material surface, the temperature field can be considered stationary for a local coordinate system of the moving laser beam. Then vaporization takes place, which ejects the material away through the assistance of inert gases, as shown in **Figure 1b**. Consequently, this causes degradation of material stiffness at elevated temperatures in the nearby cut region. A combination of necessary parameters such as power density, process speed, material properties, and beam spot diameter leads to complex interactive relations. The accuracy in the laser cutting process is highly dependent on quality characteristics of kerf width, surface roughness, heat affected zone (HAZ) width, and tensile strength, which are discussed in the following section.

3.1 Kerf Characteristics

CFRP has anisotropic and heterogeneous features and thus, making it difficult to be processed by laser. Due to this, Riveiro et al. [29] studied the cut performance of a CO₂ laser with a maximum output power of 3.5 kW in both CW mode and pulsed mode on 3 mm thick CFRP composite sheets. The processing parameters used in this experiment are laser power, cutting velocity, duty cycle, frequency of the pulse, focal length, focus position, gas pressure, nozzle diameter, and assist gas. In CW mode, they found that the kerf width increases with power. However, this results in a decrease in kerf taper angle.

In particular, the size of kerf width quadratically increases with the duty cycle, and its minimum kerf can be obtained at 50% duty cycle. In addition, increased assist gas pressure was found to cause an increase in taper angle. These findings are pretty similar to Yang et al. [30]. **Figure 2** shows the protruding fibers at the entry of the cut slot and a typical cross-section of a CO₂ laser process.

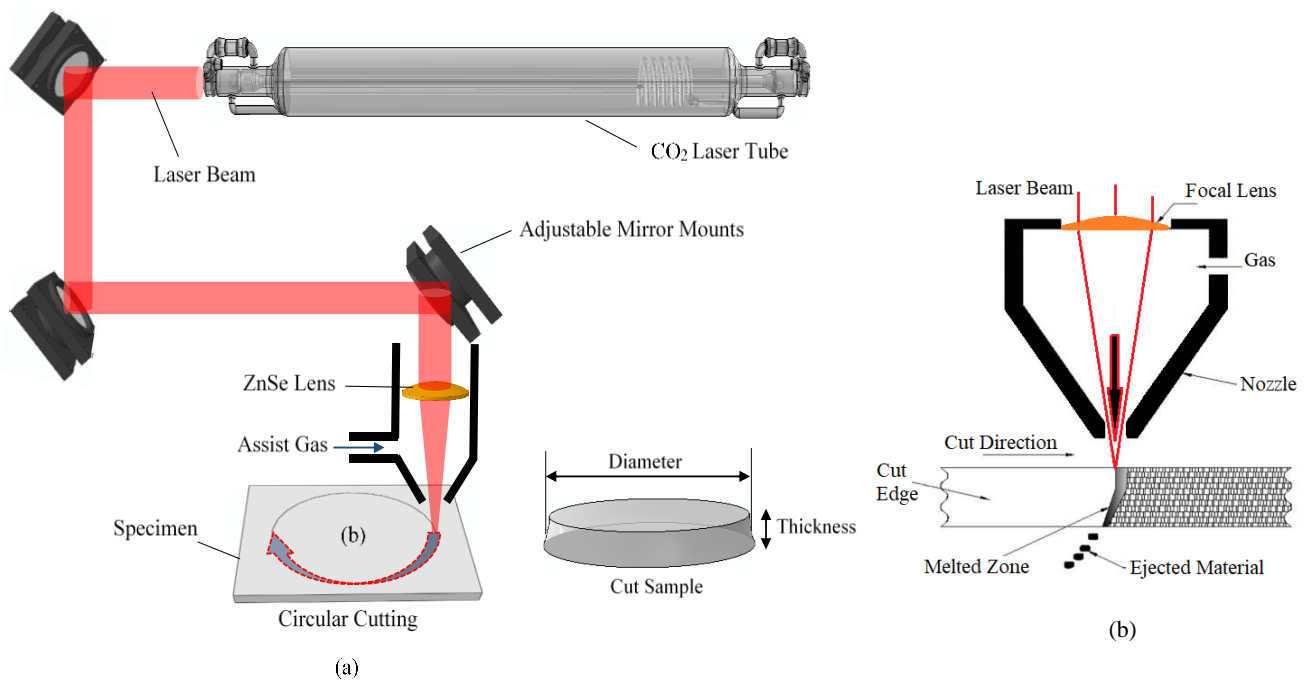


Figure 1: a) Schematic diagram of CO₂ laser cutting (adapted from Ref. [27]), b) laser beam interaction with the material substrate (adapted from Ref. [28])

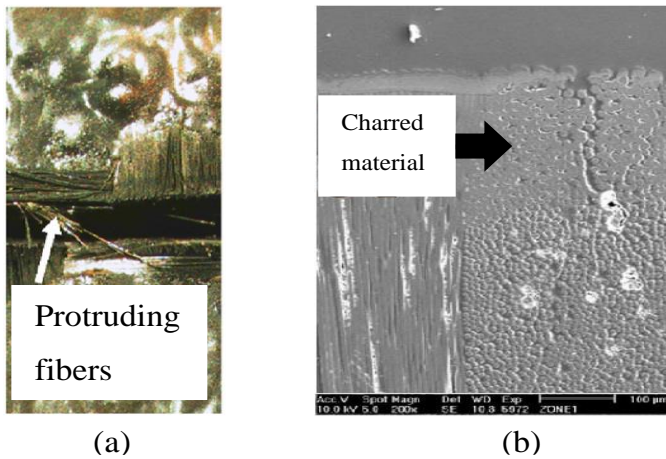


Figure 2: (a) Protruding fibers of CFRP in the entry of the cut slot and (b) SEM image of the cross-section (adapted from Ref. [29])

Moghadasi et al. [31] applied the Box-Behnken methodology to optimize low-power CO₂ laser cutting of carbon/Kevlar hybrid composite. In laser cutting of hybrid composite, the correlation between standoff distance (SOD) and other process parameters (such as laser power and cutting speed) was shown to be significant. Cutting speed and SOD substantially influenced kerf widths. In regions where the fibers are perpendicular to the cutting direction, the kerf width is narrower than in the regions where the fibers are parallel to the cutting direction.

Leone et al. [32] used Nd:YAG pulsed laser for cutting CFRP composites. Results show that the top kerf width is unaffected by the increase of spot overlap at high frequency. On the other hand, the bottom kerf width significantly decreases at high spot overlap frequency. Moreover, the kerf taper increases when the spot overlap parameter at high frequencies decreases. Staehr et al. [33] investigated laser cutting of CFRP using CW and pulsed mode. The CFRPs are made of two types of resins, epoxy (EP) and polyphenylene sulphide (PPS). They found that the kerf width generated by the pulsed mode is much broader than CW mode for both composites. In this experiment, cutting with pulsed mode requires up to 16 times more repetitions to achieve whole kerf depth than CW mode at 1.5 kW for both composites. As shown in **Figure 3**, pulsed mode for cutting CF-PPS needs less repetition rate than cutting CF-EP, whereas the number of passes in CW mode for CF-PPS is higher than CF-EP.

Tamrin et al. [34] studied low-power laser cutting of 0.4 mm CFL based on a set of experiments according to the Taguchi method. It was found that kerf width is highly affected by cutting speed. In contrast, the change of SOD has the least influence on kerf characteristics. Low laser power, high cutting speed, low number of beam passes and high SOD are essential to achieve narrower kerf width. Herzog et al. [35] studied laser cutting of 15 mm CFRP using three different methods. In the first cutting method, the laser focuses on the material's surface irrespective of the number of passes. This means that the laser remains fixed as the kerf gets deeper. On the other hand, the second method involves changing the material surface's focal position as the kerf gets deeper. In this way, the focal position remains at the material surface. Finally, the third method uses

the second method with parallel cutting at each ablation depth. The first method uses the maximum achievable kerf depth of 7.5 mm for 60 passes. For the second experiment, by retracing the focus position, the kerf width experiences double size, but there is no improvement in the kerf depth. This prevents a further increase in kerf depth because when the focused position moves inside the composite, the beam spot at the top surface increases and part of a laser beam cannot enter the pre-existent cutting groove.

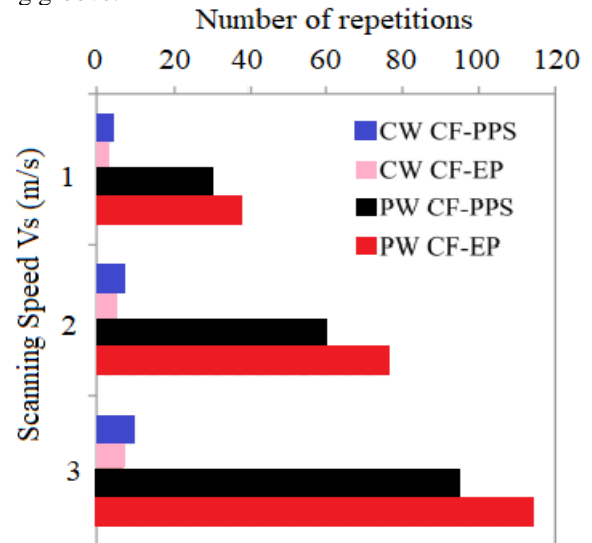


Figure 3: Comparison of the necessary number of repetitions depending on the scanning speed for CF-PPS and CF-EP (adapted from Ref. [33])

Leone et al. [36] employed a 20 kW Yb:YAG fiber laser to cut CFRP. By increasing the scanning speed up to 100 mm/s, both upper and lower kerf increase but these kerfs decrease as the speed reaches 400 mm/s. The pulse power increment leads to the upper kerf increase and the bottom kerf decrease. Furthermore, the kerf taper angle increases slightly by increasing the effective cutting speed and pulse power. Using a 1070 nm fiber laser at 400 W, Rao et al. [37] found out that the kerf width increases with the increment of laser power and gas flow rate, but it reduces with cutting speed. A similar trend is observed for kerf taper angle. Reduction in kerf width and taper angle at high cutting speed can be attributed to less interaction time between the laser beam and workpiece. In addition, the use of assist gas helps in effective material removal from the cutting zone and prevents great thermal damage but it causes larger taper angle. Ghavidel et al. [38] investigated the influence of carbon nanotubes on 120 W CO₂ laser cutting of injection moulded multi-walled carbon nanotubes/polymethyl methacrylate (MWCNT/PMMA) composite. They found that different amounts of MWCNT have various effects on kerf parameters. The increase of kerf width is linearly proportional with the increase of MWCNT, but this trend is valid up to 1 wt%. Further, increased MWCNT to 1.5 wt% results in decreased kerf width due to efficient heat conduction to the surroundings compared to the former. This also contributes to a smaller kerf taper angle. Nagesh et al. [39] investigated the influence of adding nickel nanopowder and carbon black as nanofillers in CW CO₂ laser cutting vinyl ester/glass nanocomposite. Adding more nickel nanofillers leads to

comparatively small kerf width and char reduction compared to carbon black. This is because nickel nanofillers cover the glass fibers entirely. Due to the higher thermal conductivity and lower heat capacity than carbon, they produce lower char after cutting and smaller kerf width. Niino et al. [40] studied laser cutting of CFRP using a 1090 nm 1 kW CW fiber laser. To cut through the CFRP with minimum kerf width, the power should be minimum at high cutting speed and many passes. The number of passes is greatly dependent on material thickness. These findings agree with other literature results [29, 36, 37, 41, 42]. Nattapat et al. [43] studied the possibility of removing the top resin layer of CFRP using a 60 W CO₂ laser. The results demonstrate that increased laser power and decreased cutting speed lead to more ablation of resin and fiber damage and deeper kerf depth. Negarestani et al. [44] investigated CFRP laser cutting using Nd:YVO₄ ultraviolet laser. Thermal damage and ablation depth decrease with the increase in cutting speed, leading to shorter fiber pullout. At high cutting speed, more passes are needed to achieve through a cut. Similarly, the results of Salama et al. [45] showed an increased ablation rate at high energy and repetition rate using a 250 kW CO₂ laser. Using picosecond pulsed laser radiation, Finger et al. [46] noted an increased ablation rate due to superimposed laser pulses and consequently accumulated heat in the localized region. Wu et al. [47] favoured shorter pulse duration to achieve minimum kerf taper at certain ablation depth in their experiment. Finally, Yang et al. [30] demonstrated a faster ablation rate using Nd:YAG pulsed laser at the expense of larger HAZ due to insufficient cooling time.

Fürst et al. [48] employed CW CO₂ laser and CW Nd:YAG to cut glass fiber -reinforced thermoplastics. Two beam radiations with 1.09 and 10.6 μm wavelengths were simultaneously applied. They discovered that a single CO₂ laser generates the widest kerf compared to alternative proportions of combined laser beams and a single Nd:YAG laser. The evaporation of a significantly larger volume of material removal and bigger kerf can be attributed to the larger spot diameter of the CO₂ laser. In contrast, the narrow beam and high intensity of the Nd:YAG laser produced small kerf width. Choudhury et al. [49] investigated the cutting quality of GFRP by using single -pass and double -pass techniques of 500 W CW CO₂ laser. The

results depict that the upper kerf width increases with the increase of assist gas nozzle diameter for the single pass beam. However, it decreases when the material thickness and cutting speed increase. Additionally, lower kerf width decreases with the increase of nozzle diameter, material thickness and laser cutting speed. The same result can be observed in the double pass beam, but the difference is that the double pass beam generates lower kerf width than the single pass beam. Adalarasan et al. [50] studied the cutting process of Al6061/SiCp/Al₂O₃ metal matrix composite using a 3.8 kW pulsed CO₂ laser. They found that minimum cross height and decreased kerf width can be obtained at high nitrogen gas pressure due to the easy ejection of molten metal. In contrast, the combined effect of higher pulse energy at high frequency and lower cutting speed causes overlapping of successive beam spots and re-solidification of the overlapped regions, which in turn ruins the surface finish. Similarly, higher cutting speed and high pulse energy result in poor finish cut due to less interaction time between the material and laser beam. Therefore, a modest cutting speed (19.94 mm/s) was found acceptable for better kerf and the quality of the cut. Tong et al. [51] studied the ablation behaviour of the C/SiC composite using a Nd:YAG pulsed laser. During the laser process, the composite absorbs the laser energy due to absorption rate, surface heat conduction and the trapping laser beam in the ablated region. As a result, the ablation rate of the composite increases linearly with laser power, as seen in **Figure 4a**. In contrast, **Figure 4b** shows that the ablation rate decreases linearly with prolonged ablation time. The reason may be explained in two aspects. Firstly, due to the increased distance between the laser focal point and the ablated surface of the composite, the temperature generated by the laser beam decreases. On the other hand, forming a positive pressure during the ablation process may result in scattering the laser beam and entraining much heat to the ablation surface. The PMMA substrates were experimented with Prakash et al. [25] to fabricate microchannels using multi-pass CO₂ laser cutting. The multi-pass technique at higher cutting speeds compared to single -pass at lower values produces reduced kerf width. However, kerf width generally increases with the increase of laser power.

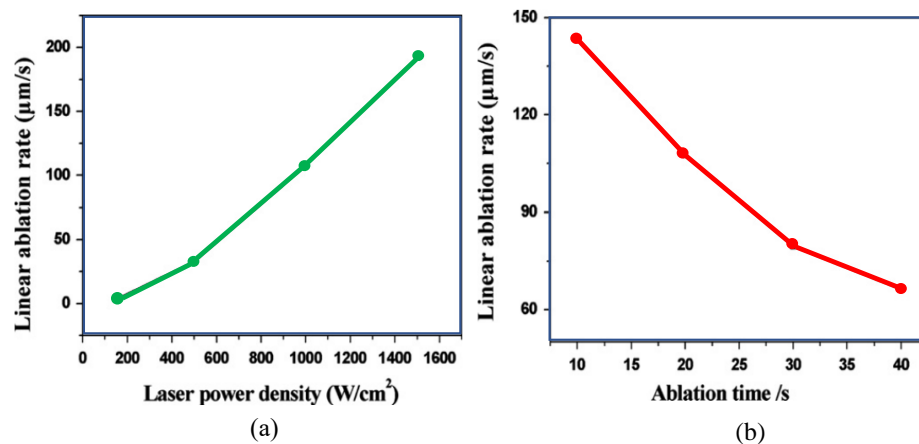


Figure 4: (a) Linear ablation rates of the C/SiC composite at different laser power densities, (b) Linear ablation rates of the C/SiC composite versus the ablation time at power density 1000 W/cm² (adapted from Ref. [38]).

Their other research [52] discovered that as the number of pulses per linear inch (PPI) decreases, the pulse's average energy is increased compared to a higher PPI. This is due to the distribution of energy in a lesser number of pulses. Therefore, the largest width is achieved when the highest power is united with the lowest speed and the smallest PPI. In addition, when the scanning speed increases, the microchannel width becomes narrower. It is evident that the increase in velocity leads to reduced energy transfer per unit length to the material. In addition, when the pulse overlap decreases, energy accumulation per unit area decreases, resulting in a narrower channel.

In a similar work, Chen et al. [53] examined the effect of CO₂ laser processing on the microchannel fabrication of PC substrate. The orthogonal experiment approach was successfully implemented for channel width optimization. The results indicated that laser power significantly influences width, while the effect of cutting speed is the least.

3.2 Surface Roughness

Takahashi et al. [54] studied the effect of hatching distance for cutting CFRP using a 1064 nm 125 W fiber laser. It was discovered that the ejection of ablated material at higher values of hatching distance is very smooth, resulting in lower surface roughness, especially at higher scanning speeds. **Figures 5a** and **5b** show SEM micrographs of groove walls at 2.75 m/s and 11 m/s scanning speeds with a similar hatching distance of 250 μm , respectively. The increased cutting speed decreases the surface roughness efficiently and creates a smoother cutting surface. **Figures 5c** and **5d** show the cross-sectional profile obtained for cutting speeds of 2.75 m/s and 11 m/s, respectively. In addition, **Figure 5e** shows the dependence of the surface roughness Ra on the hatching distance for scanning speeds of 2.75 and 11.0 m/s, which provides quantitative support for **Figures 5a** to **5d**. Surface roughness decreases with the increase of hatching distance up to 150 μm , but its effect is negligible beyond this value. The increased hatching distance results in easier laser light penetration into the CFRP and reduced heat accumulation.

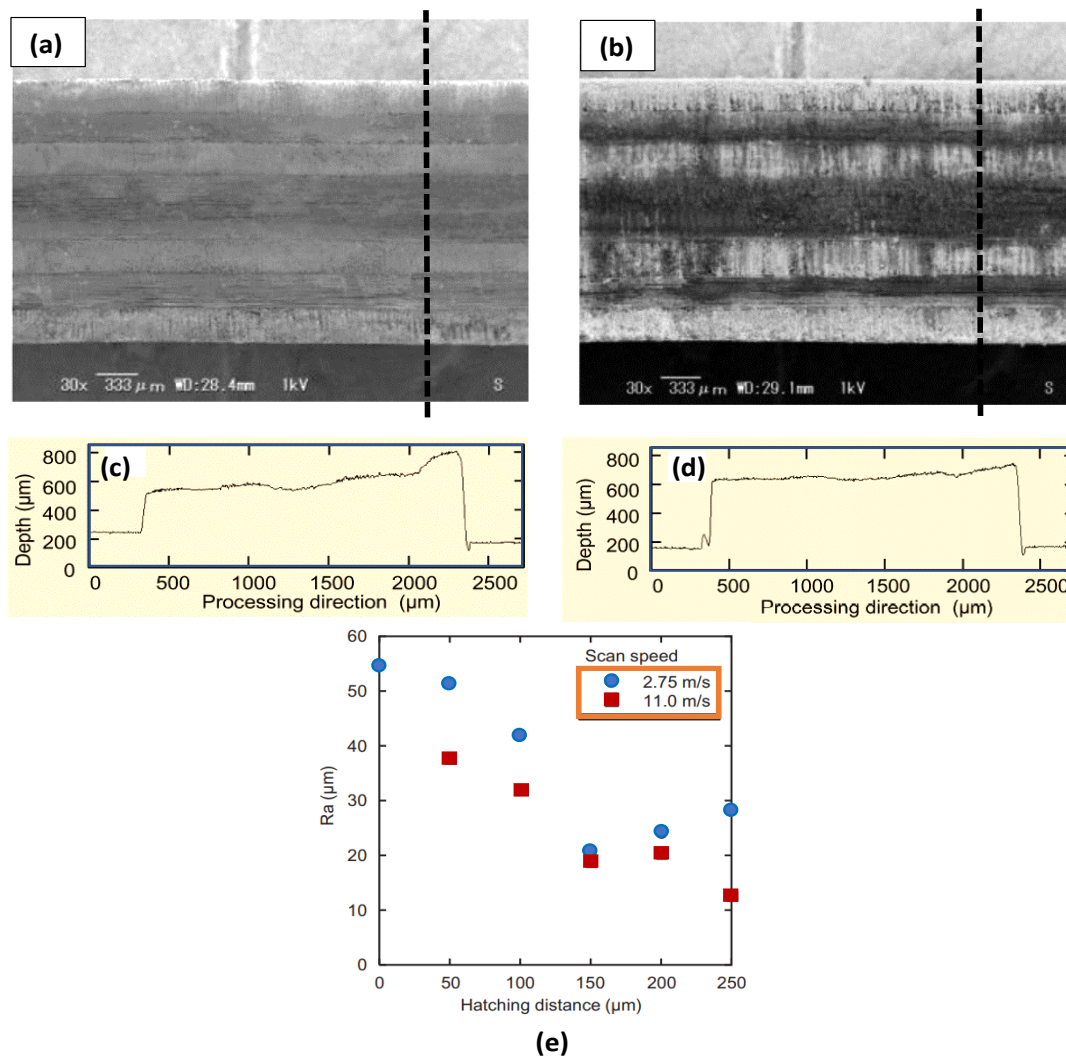


Figure 5: (a) and (b) SEM micrograph of the groove walls after irradiation with laser light for 250 μm hatching distance at the scanning speed of 2.75 m/s and 11 m/s, (c) and (d) Cross-sectional profiles of CFRP processed at the location indicated by the dotted line at scanning speed of 2.75 m/s and 11 m/s, (e) Surface roughness Ra as a function of the hatching distance for scanning speeds of 2.75 and 11.0 m/s (adapted from Ref. [54]).

Karimzad Ghavidel et al. [55] investigated the effects of adding carbon nanotubes inside the MWCNT/PMMA nanocomposite. The result shows the increase of surface roughness with the increase of carbon nanotubes percentage. This is because a higher percentage of carbon nanotubes improves laser-material absorptivity and decreases thermal conductivity [39, 56]. The reduction in thermal conductivity of the nanocomposite causes the solidification of melted material on the surface, roughening the cut surface. Furthermore, laser power and cutting speed have negligible influence on surface roughness.

Choudhury et al. [49] discovered that the surface finish of GFRP in double-pass CO₂ laser cutting is better than single-pass mode. This is because, in single-pass mode, the cutting speed was set at a low pace to allow through the cut, which causes a charred surface. On the contrary, in double-pass mode, the cutting speed was set at a relatively high pace which positively led to a smoother surface and no burnt region. Furthermore, the effect of assist gas nozzle diameter on surface roughness was also investigated in both cutting modes. It was found that the nozzle diameter has an insignificant effect on the surface roughness in the single-pass laser beam. However, the effect of changing nozzle diameter is more pronounced in double-pass, especially at low cutting speed.

Nagesh et al. [39] found out that by adding nanofillers (nickel and carbon black) to the FRP nanocomposites (vinyl ester/glass), surface roughness and quality of surface cut can be improved. Nickel nanopowder produces a smoother surface and better cut quality than carbon black due to its higher thermal conductivity and lower heat capacity. This effectively improves heat dissipation and reduces char formation. Furthermore, it was found that char content directly influences surface roughness, in which lesser char was observed for composite added with nickel nanofillers.

Adalarasan et al. [50] demonstrated the use of nitrogen assist gas at high pressure for easy ejection of molten Al6061/SiCp/Al₂O₃ metal matrix composite in pulsed CO₂ laser cutting. This minimizes dross and improves surface roughness.

3.3 Heat Affected Zone (HAZ)

Leone et al. [32] studied laser cutting of CFRP using Nd:YAG pulsed laser. They found that high pulse energy at low frequency and high cutting speed lead to lower HAZ. On the contrary, larger HAZ was obtained for low pulse energy at high frequency and low cutting speed. The maximum HAZ extension occurs at the centre of the laminate in the range of 170-1600 μm. The optical microscopy analysis in **Figure 6** shows typical composite thermal damage, such as fiber pullout, matrix recession, matrix thermal degradation and carbonisation of both matrix and fiber. **Figure 6a** shows the outer top laminate side, obtained at high pulse energy and low frequency. The visible damage extension on matrix and fiber was noticed due to directly exposed of CFRP to the laser radiation. **Figures 6b** and **6c** show the effect of high frequency and low cutting speed on HAZ extension and degradation of fibers and carbonisation of the matrix, resulting in fiber pullout. The effect of low - power laser cutting of cotton fiber laminate on HAZ was discussed by Tamrin et al. [34]. It was discovered that laser cutting speed is the most influential parameter on HAZ,

affecting interaction time between the laser and the sample. A similar result was shown in other research findings [57, 58].

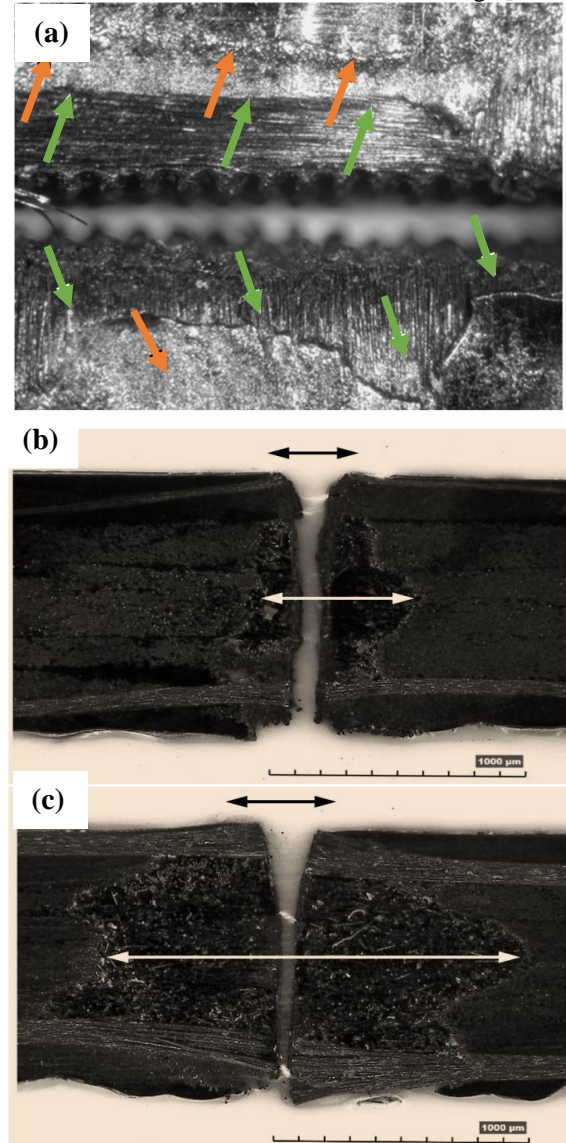


Figure 6: (a) Matrix recession (green arrows) and burnings (orange arrows) at the top kerf, (b) HAZ extension at pulse duration 0.25 ms, frequency 140 Hz and scanning speed 12.5 mm/s, (c) HAZ extension at pulse duration 0.05 ms, frequency 1790 Hz, scanning speed 6 mm/s (adapted from Ref. [32]).

Considerable increases in HAZ were reported in [31] due to increased absorption of thermal energy and longer laser-material exposure at high laser power and low cutting speed in CO₂ laser cutting of carbon/Kevlar hybrid composite. In addition, the adjacent region to top kerf width showed a complete vaporization of epoxy due to significantly low thermal decomposition of matrix (epoxy) as compared to both fibers. Also, due to the lower thermal conductivity of Kevlar fibers and high heat absorption, the charring and swelling of Kevlar fibers occurred, resulting in a completely burnt and brittle region.

Yang et al. [30] evaluated the effect of Nd:YAG pulsed laser cutting quality of CFRP. They discovered that HAZ increases

with the increase of pulse frequency, pulse duration and pulse energy. The increase of pulse frequency and duration has an effect similar to a laser operating in continuous mode.

Staehr et al. [33] studied the influence of two types of lasers for cutting CFRP; a single-mode fiber laser emitting continuous waves and a high-power thin disk laser emitting nanosecond pulses. They figured out that the former produces small HAZ at low cutting speed, whereas the latter produces small HAZ at high cutting speed. Herzog et al. [35] experimentally studied cutting of 15 mm CFRP. They used three methods. In the first method, the laser is focused on the material's surface regardless of the number of passes. In the second method, the focal position changes proportionally relative to the material surface as the kerf gets deeper. Finally, the third method uses the second method with parallel cutting at each ablation depth. Overall, the HAZ is unaffected by all these three methods.

Bluemel et al. [59] investigated two HAZ measurements using thermography for surface temperature and thermocouples for internal body temperature. The measured temperature at the specified distances from the cutting edge by these two methods states that the HAZ decreases when the distance from the cutting region increases. This trend is similar for both surface and internal body of the composite. Thermography is generally more appropriate for HAZ measurement than thermocouples due to its non-contact method. Xu et al. [60] studied the effect of HAZ after cutting CFRP using a Nd:YVO₄ nanosecond pulsed laser system. It was observed high overlapping rate and low scanning speed can contribute to large HAZ at the expense of reduced machining efficiency.

Riveiro et al. [29] studied the effect of both CW and pulsed CO₂ laser on the cutting quality of 3 mm CFRP. In CW mode, the power increase leads to the increase of HAZ. Similarly, the increase in the duty cycle causes an increase in HAZ. However, it was found that the increase in assist gas pressure does not significantly affect the reduction of HAZ. Furthermore, due to the high thermal conductivity of carbon fibers and the conduction of heat along the fibers, the extent of HAZ in cutting perpendicular to the fiber axis is greater (Herzog et al. [61]).

Takahashi et al. [62] investigated cutting parameters of CFRP using Nd:YAG laser for both ultraviolet (UV- $\lambda=266$ nm) and infrared (IR- $\lambda=1064$ nm). They found that HAZ produced by IR irradiation is wider than by UV irradiation. This is because IR laser irradiates the laser beam to pass through the resin and is subsequently absorbed by the carbon fibre underneath the resin. In contrast, UV light heats only the resin surface. Hence, heat propagation in the former case is comparatively larger than that of the latter, producing greater HAZ. Jaeschke et al. [41] investigated the impact of thermal damage on cutting CFRP using a 6 kW fiber laser. At constant laser power of 6 kW, they found that HAZ width decreases with the cutting speed increase. On the other hand, by altering the laser power at a constant cutting speed, the width of HAZ remains constant. Furthermore, they showed a decrease in HAZ increases the tensile strength [61, 63, 64].

Leone et al. [36] did experiments on laser cutting of CFRP using a Q-Switched Yb:YAG fiber laser. They found that the increment of either scanning speed or pulse power contributes to a decrease in HAZ. The reason is that the increase in scanning

speed allows better cooling of the composite and, consequently, reduces the cutting temperature. Similarly, increased pulse power allows efficient material removal and mitigates heat conduction and absorption to the neighbouring regions. All these effects contribute to a reduction in HAZ.

Muramatsu et al. [63] investigated HAZ's effect on CFRP's tensile strength. They used three different types of lasers; (1) a CO₂ laser ($\lambda = 10.6$ μm) with a processing speed of 1.0 m/min and a power of 800 W, (2) a single-mode fiber laser ($\lambda = 1.06$ μm) with a processing speed of 1.0 m/min and a power of 350 W and (3) a single-mode fiber laser ($\lambda = 1.06$ μm) with a processing speed of 7.0 m/min and a power of 2 kW. The fiber laser produces the lowest HAZ when set at high laser energy and cutting speed [36]. This favourably results in high tensile strength [41].

Herzog et al. [65] studied the effect of 30 kW Yt:YAG fiber laser on cutting CFRP by separately applying one-pass and multi-pass strategies. They obtained a minimum HAZ of 139 μm in a single pass strategy at maximum power and maximum cutting speed of 1.2 m/s. On the contrary, in the multi-pass strategy, the optimum passes required to acquire minimum HAZ (78.3 μm) is 12. The increase in the number of passes results in a steep increase in HAZ. Furthermore, decreasing the delay time below 100 ms between 2 passes causes a sharp increase in HAZ. The same trend can be observed by decreasing the interaction time between the material and the laser beam below 10 μs [32, 36, 66].

Takahashi et al. [54] studied the effect of hatching distance on the cut quality of CFRP using 125 W pulsed fiber laser. It was observed HAZ decreases when both hatching distance and scanning speed increase. This is because a narrower hatching distance causes heat accumulation inside the groove and, consequently, an increase in HAZ. On the other hand, a larger hatching distance allows easier penetration of the laser light into the substrate and reduces heat accumulated inside the groove. As a result, the measured HAZ is significantly smaller.

Karimzad Ghavidel et al. [55] studied the effect of a 130 W CO₂ laser on the cutting quality of MWCNT/PMMA nanocomposite. The nanocomposite was fabricated using an injection moulding technique where carbon nanotubes are usually aligned in the direction of flow injection. The increase in MWCNT percentage leads to the increase of HAZ and the burr in the direction of flow injection. Similarly, the power increase results in larger HAZ and burr. On the other hand, HAZ and burr increase by increasing the MWCNT percentage perpendicular to the flow injection. In the latter case, HAZ is comparatively unchanged but burr decreases with increased laser power. The increased cutting speed leads to the decrease of HAZ and burr for both carbon nanotube alignments.

Rao et al. [37] studied the effect of laser cutting parameters on the cut surface integrity of CFRP. It was observed that the HAZ increases when the laser power and assist gas increase. In addition, the HAZ decreases when the cutting speed increases due to less exposure time. As a result, the melting zone adjacent to HAZ appears narrower.

Ghavidel et al. [38] investigated the effect of carbon nanotubes on the laser cutting of MWCNT/PMMA nanocomposite using a 60 W CW CO₂ laser. Thermal conductivity was found to

increase with the amount of carbon nanotube percentage. This resulted in HAZ decrease when the laser power and cutting speed increased.

Salama et al. [32] investigated the effect of a 250 kW CO₂ laser with a short pulse duration (8 μs) on the cut quality of CFRP. Qualitative observation indicates that a faster scanning speed results in less energy input per unit length to the material, thereby reducing HAZ. They discovered that a lower scanning speed results in a prolonged laser-material interaction time and higher spot overlaps, which leads to a relatively high HAZ. Interestingly, the HAZ was found minimum at high scanning speed and low/high repetition rate. They demonstrated better quality and lower HAZ than those using continuous CO₂, fiber, and Nd:YAG lasers [44, 67].

Using a picosecond pulsed laser, Finger et al. [46] found that the width of HAZ is smaller for a lower repetition rate. The cause of this effect is that the applied energy for the ablation process is superimposed by the accumulation of heat due to the overlap of laser pulses. However, the HAZ is significant at a high repetition rate, contrary to the finding in [45]. Furthermore, it is noted that HAZ decreases at higher scanning speeds, but remains constant at a repetition rate between 200 kHz to 500 kHz. Niino et al. [40] investigated the effect of a multi-pass CW IR fiber laser ($\lambda=1090$ nm) on cutting 3 mm thick CFRP. A linear relationship exists between cutting depth and the number of passes at varying scanning speeds. In addition, small HAZ was obtained at high scanning speed due to minimum thermal decomposition of the resin and lesser heat accumulation in that region.

Patel et al. [68] studied the effect of laser input parameters: velocity of cutting, laser power and gas pressure towards HAZ in GFRP composites. This study used a fiber laser with a maximum output power of 2 kW to cut the material. Second Order Regression and Artificial Neural Network (ANN) modeling techniques were developed for optimization and result prediction. They found that cutting speed has the most crucial effect on HAZ compared to laser power and gas pressure. The workability of the developed models was checked by comparing the predicted results with the experimental results that ANOVA conducted. After comparing, the results showed that the ANN model has better accuracy than the Second Order Regression model for HAZ prediction.

The same finding was shown by Moghadasi et al. [31] in multi-pass CO₂ laser cutting of carbon/Kevlar hybrid composites. The effect of laser processing parameters was discussed using ANOVA and response surface methodology. It was indicated that due to increased absorption of thermal energy and longer laser-material exposure at higher laser power and lesser cutting speed, the HAZ increases significantly. On top of that, the minimum HAZ was observed when SOD was equivalent to the focal length at the smallest beam spot.

Fatimah et al. [69] investigated beam cutting of GFRP composite by using 30 W of CO₂ laser. In this experiment, the focal length of the focused beam was varied to obtain the beam's different spot sizes. The smallest focus spot size is achieved when the focal length is 9.5 mm. The surface quality of the material was also investigated. Burn marks and HAZ occurred during the cutting process. This is because the profile

of the material is affected by the variation of the beam intensity. In the experiment, it was also found that focal length also affects the depth and removal rate of the composite. However, only minor changes in the depth and removal rate of the composite occurred due to the fiber compound that prevents the beam intensity. Hence, they concluded that other laser input parameters, such as laser power, cutting velocity and assist gas pressure, should be included in the laser processing of polymer composite.

To find the optimum process parameters in CO₂ laser cutting of PMMA, PC and PP, Tamrin et al. [70] utilised grey relational analysis. The results correspond well with the findings in the literature, where a precise cut dimension is attributed to minimum HAZ. Further analysis using ANOVA indicated that laser power has a pronounced impact on HAZ amongst the other process parameters, such as cutting speed and air pressure; this applies to all thermoplastics.

Prakash et al. [25] discovered that multi-pass CO₂ laser processing for fabricating microchannels using PMMA substrates significantly minimizes HAZ at higher cutting speeds. In contrast, the power increase at a lower number of passes causes more swellings on the top of the workpiece owing to low thermal conductivity and heat accumulation. **Figures 7a** and **7b** show the effect of the multi-pass technique in considerable HAZ reduction. The bar graph in **Figure 7c** also represents the HAZ variation in different numbers of passes for a 500 μm depth microchannel. The value of HAZ in one-pass processing is twofold compared to 7-pass. Additionally, when two-pass laser processing was performed, an abrupt decrease in HAZ was observed.

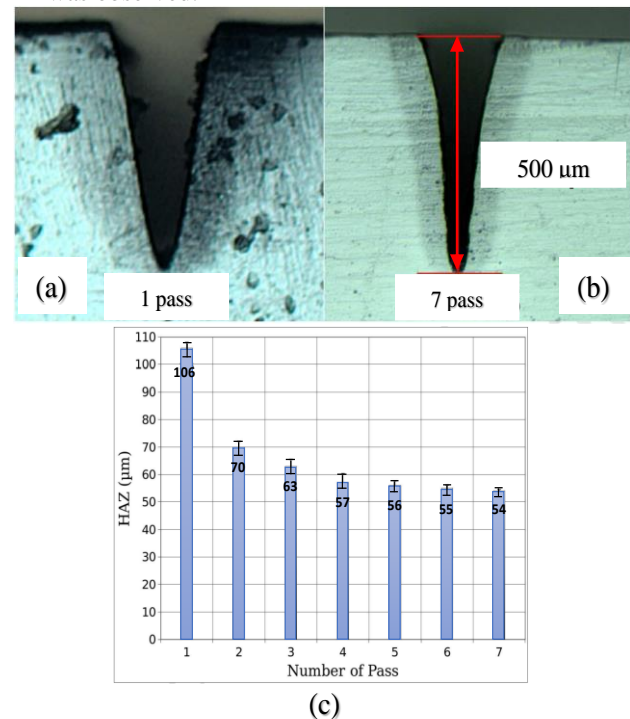


Figure 7: (a), (b) HAZ in a 500 μm depth microchannel resulting from 1-pass and 7-pass, (c) HAZ for a 500 μm depth microchannel fabricated in different number of passes (adapted from Ref. [25])

3.4 Mechanical Strength

Jaeschke et al. [41] studied the impact of thermal damage of a 6 kW fiber laser on the tensile strength of CFRP., The thermal damage in the interlaminar section due to laser cutting reduces maximum shear stress compared to conventional methods (milling and abrasive water jet). While varying the laser power from 550 W to 6 kW at a constant feed rate of $v=1.2$ m/min, it was observed that the output power has a minor effect on the static tensile strength. At constant power of 6 kW, the tensile strength increases by 25% by increasing the feed rate from 1.2 m/min to 13.1 m/min.

Herzog et al. [61] studied the static strength of CFRPs cut using three different laser sources: a pulsed Nd:YAG laser, a disc laser and a CO₂ laser. They found out the values of static- or bending strength produced by laser methods are far above as compared with conventional machining methods. Moreover, the pulsed Nd:YAG laser produces the highest strength having the smallest HAZ in which there exists a linear relationship between the width of the HAZ and the tensile strength (Jaeschke et al. [41]). Results show the fiber orientation can influence the static strength, reducing by about 84 MPa and 35 MPa for a fiber orientation of 90° and 45°, respectively. This implies that static strength effectively decreases with the increase of the degree of orientation and HAZ.

Muramatsu et al. [63] reported a reduction in stress and an increase of HAZ in the laser cutting of CFRP sheets using three laser types. In comparison, the strength of CFRP specimen cut by 2 kW fiber laser is better than that of 800 W CO₂ laser and 350 W fiber laser.

4. Numerical Simulation

The distribution of temperature generation, stress propagation, and HAZ significantly affect the laser cut quality. Since the cutting process is incredibly fast, the underlying transient process is challenging to measure. Therefore, a complete numerical simulation could help reveal invaluable information upon validation. Numerical simulation can be divided into three different techniques, finite element method (FEM), finite difference method (FDM), and finite volume method (FVM). The simulation techniques help in the development of thermal loading and predict the temperature profile as well as the following thermal stress fields. The standard mathematical formulation of the transport equation for heat transfer applicable to laser heating of the workpiece may be written as [27, 71-73]:

$$\rho \frac{dC_p T_i}{dt} = \nabla(K \nabla T) + Q - Q_v \quad (1)$$

where ρ is the density of the material (kg/m³), C_p is the specific heat capacity (J/kgK), T_i is the temperature (K), t is time variable (s), K is the thermal conductivity (W/mK), Q is the heat source and Q_v is the heat loss due to heat convection. At the surface of specimens, convectional heat transfer and radiant heat transfer are responsible for the heat loss, considering other free surfaces to be adiabatic.

High-temperature gradients along the cutting edges cause the development of a significant stress field in the cutting region. Once the stress rates approach critical values, the loss of strength and the creation of initial cracks at the cutting edge are unavoidable, limiting the practical applications of the machined

components. In addition, the stress distribution may be determined by utilization of the temperature field as an input for mechanical analysis. Thus, the element type must be altered to a transient stress analysis considering the strain caused by thermal loading.

The stress is related to the strain by:

$$\{\varepsilon\} = C^{-1}\{\sigma\} \quad (2)$$

where $\{\sigma\}$ is the stress vector, C is the stiffness matrix, and $\{\varepsilon\}$ is total strain vector. The total strain tensor can be written as:

$$\{\varepsilon\} = \{\varepsilon^{el}\} + \{\varepsilon^{pl}\} + \{\varepsilon^{th}\} \quad (3)$$

where $\{\varepsilon\}$ is total strain vector, $\{\varepsilon^{el}\}$ is elastic strain vector, $\{\varepsilon^{pl}\}$ is plastic strain vector, and $\{\varepsilon^{th}\}$ is thermal strain vector.

4.1 Finite Element Method (FEM)

Moghadasi et al. [27] investigated the effect of CO₂ laser cutting on different thermoplastics. The numerical results agreed correctly with the experimental findings. An uncoupled thermo-mechanical technique was employed to achieve temperature gradients and stress distribution. Damage properties were defined according to the strength loss at high temperatures. Therefore, element deletion was activated, resulting in kerf characteristics and HAZ measurement. It was indicated that the increased cutting speed decreases the temperature gradient at the same laser power. It was also shown that PC undergoes a higher temperature profile than PMMA and PP. This is due to its higher specific heat and thermal conductivity at higher temperatures than PMMA and PP. **Figure 8** shows the temperature field and stress distribution at the last time increment of PC laser cutting. It was found that temperature decay along the cutting edges is relatively gradual through conductive and convective modes of heat transfer [74, 75]. von Mises stresses were seen to have a higher magnitude in the region of high -temperature gradient, especially the adjacent cutting region. It was shown that due to decreasing the elastic modulus of the workpiece by the rise of temperature, elements lost their strength correspondingly and were deleted from the region exposed directly to the Gaussian laser beam. In their other study [71], they studied the effect of multi-pass CO₂ laser cutting of carbon/Kevlar hybrid composite using finite element method. It was indicated by multi -pass technique, the heat accumulation of the preceding passes resulted in remaining residual temperatures after the second and third passes. Because carbon fibers have a higher thermal conductivity than Kevlar fibers, the temperature gradient surrounding the fibers is not uniform. In addition, stress profiles revealed that stress rises typically as the number of passes increases.

CO₂ laser cutting of PC was investigated by Moradi et al. [76], employing both the finite element method and statistical techniques of variance analysis. The laser heat flux was simulated in ABAQUS using the DFLUX subroutine. The results revealed that the laser scanning speed majorly affects the kerf characteristics. On the contrary, decreasing HAZ is shown prominently by increasing laser cutting speed and reducing laser power. Experiments and numerical modeling showed consistent findings, demonstrating the simulation accuracy with a maximum error of less than 12 percent.

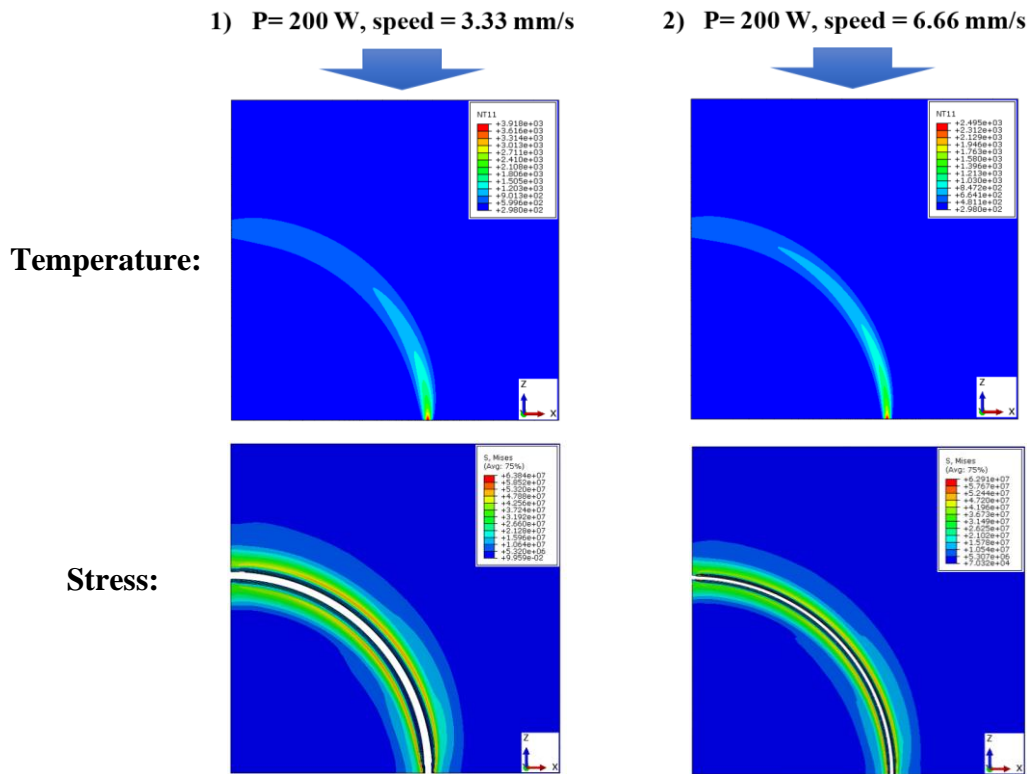


Figure 8: Temperature and stress gradients for PC at laser power 200 W and different cutting speeds, 1) $v = 3.33$ mm/s, 2) $v = 6.66$ mm/s [27]

Negarestani et al. [44] established a new technique using FEM to simulate transient temperature during laser cutting of CFRP. The change in spacing distance of laser tracks was investigated as a critical factor influencing ablation depth and HAZ.

All surfaces are considered adiabatic except the top surface and the groove side. Increasing the cutting speed causes a decrease in the thermal damage, HAZ and ablation depth which favorably leads to shorter fiber pullout.

Nattapat et al. [43] employed FEM analysis to investigate the likelihood of removing the top resin layer of the CFRP sheet. Experiments and FEM were conducted using laser powers (8 W, 14 W and 20 W) and a cutting speed of 880 mm/s. The FEM model used in this work was formulated based on the heat conduction equation previously developed by Negarestani et al. [44]. They discovered that fibers are not damaged when the power is less than 8 W. It is feasible to remove resin without damaging the layers if the power is between 8 W and 20 W. When the laser energy exceeds 20 W, the substrate damage is more evident. At a laser power of 14 W, they determined that a beam overlap of 25% produces the best surface characteristics without causing damage to the layers.

Wu et al. [47] performed simulated ablation behaviour of CFRP using three different laser operation modes: continuous wave, long -duration pulsed wave (LP) and short -duration pulsed wave (SP) lasers. Comparatively, the short -duration pulsed laser did not lead to much ablation. Numerical computation shows that the peak temperature developed by CW laser was stabilized around the sublimation point of epoxy. For the cases of a pulsed laser, first pulse resulted in ultra-high temperature

(over 25,000 K) in the top carbon fabric layer. Then the temperature returned and stabilized around the epoxy matrix's sublimation point soon after the pulse's end.

By studying the interlaminar damages of CFRP during CO₂ laser cutting, Liu et al. [77] employed FEM analysis to calculate the interface stress. The previously adopted heat conduction equation and thermal boundary conditions by Wu et al. [47] were utilised to perform this analysis. By elevating the laser power from 500 W to 1000 W, the position of the significant cracks was shifted to the rear surface. Due to an increase in maximum normal and shear loads at the interfaces of the lamina, the number of interlaminar fractures rises when the laser power is increased.

Sun et al. [78] investigated the 'Element birth and death' technique in single-pass laser cutting of unidirectional CFRP with and without the assistance of waterjet. The former case produced lesser HAZ extension along with shallower ablation depth. Furthermore, the HAZ remained consistent despite various cutting speeds due to the waterjet's practical cooling function. In contrast, for the latter case, increased cutting speed reduced damage caused by laser heat.

Yilbas et al. [74] employed finite element modeling to predict the developed thermal-stress field in the cutting zone of KFRP under the premise that KFRP acts as an elastic-plastic (isotropic) material. The projected temperatures correlated well with the thermocouple data and were found to be high around the kerf edge and its surroundings, significantly declining as the distance from the cut zone increased. As the temperature gradient evolves, thermal strain increases, resulting in a

substantially elevated von Mises stress. Following work in [74], the measurement of temperature and stress field in the circumference of the cutting region was simulated by Yilbas et al. [75] by adopting circular laser cutting of KFRP. It was established that the temperature keeps rising throughout the circle of the cutting edge and progressively gets lower values along its thickness. In addition, the maximum temperature value estimated for the larger diameter hole is higher than that of the smaller diameter hole, owing to the shorter time required to cut the latter. Therefore, the von Mises stress of the former is somewhat increased. Long et al. [79] examined the temperature distribution of the ablated zone of CFRP by considering a radially symmetric laser beam and the 'element birth and death' approach. Based on the irradiated zone's expected peak temperature (2950 °K), elements on the ablated region can be removed in this fashion. Simulation and experiment showed similar characteristics of the ablated area.

4.2 Finite Difference Method (FDM)

Xu et al. [60] used the finite difference method (FDM) to model the ablation of CFRP using single and consecutive short laser pulses. They found that high overlapping rate may cause a reduction of the machining efficiency and enlargement of HAZ. On the other hand, by increasing the power, the ablation depth increases.

4.3 Finite Volume Method (FVM)

Ohkubo et al. [80] performed a three-dimensional numerical simulation of cutting CFRP using the finite volume method (FVM) by Open-Foam. A simplified equation model that considers the CFRP thermal conduction as a time-dependent heat conduction equation was used (Negarestani et al. [44]). Carbon fiber can be eliminated faster than resin at the first stage due to the difference in thermal conductivity. Removal of resin is attributed to its low combustion temperature. **Figure 9** shows the removed length for both fiber and resin. Although longer removed length is observed for carbon fiber before 28 μ s, it is seen that the removing length of epoxy resin becomes longer than carbon fiber after this time. This timing, firstly, clarifies the same existence of the removed length of carbon fibers and epoxy resin and secondly, becomes the optimal time contacting ablation plume and kerf of the target. Consequently, laser ablation should be omitted after laser irradiation meets this result.

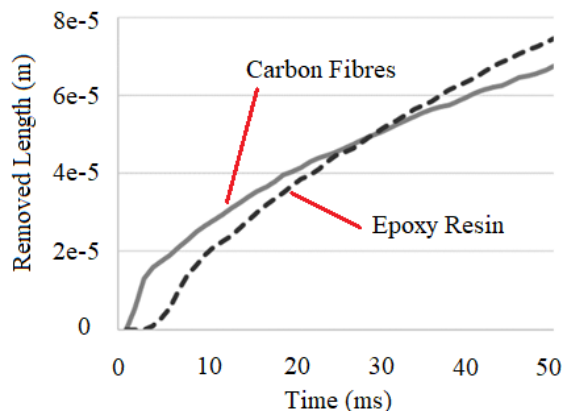


Figure 9: Removed length for both fiber and resin (Adapted from Ref. [80])

Conclusions

Numerous types of research have been conducted on laser beam cutting of composites and thermoplastics, either experimentally or numerically. Based on what has been discussed in the preceding sections, the following conclusions can be drawn:

- 1- The significant input process parameters that influence laser cut quality include: material properties (type, thickness), laser parameters (laser power, wavelength, mode of operation), and process parameters (pulse frequency, pulse width or duration, cutting speed, focal plane position, pulse energy, travel direction, assist gas type and pressure).
- 2- The cut quality of laser -processed materials can be predicted using DOEs and various artificial intelligence -based techniques.
- 3- The optimum process parameters based on laser cut quality characteristics (such as kerf width, HAZ, and surface roughness) can be determined using single and multi-objective optimization techniques.
- 4- In order to reduce HAZ, it is recommended to use ultra-short pulses, high values of cutting speeds, multi-pass strategy, low beam intensity, and high -pressure assist gas.
- 5- Surface roughness is significantly influenced by cutting speed. In addition, better surface quality is found in the cutting region by employing inert gases.
- 6- The multi-pass processing technique with appropriately adjusted scanning speed and interval times between the scans may result in good productivity with high -quality cut edges.
- 7- Numerical modeling offers surface temperature and residual stress predictions, which agree well with their corresponding experimental analysis in the cut section. Analytical modeling and simulation in laser beam machining can reliably predict the cut quality characteristics for various input parameters.

Acknowledgement

This work was supported by the Ministry of Higher Education Malaysia through Fundamental Research Grant Scheme (FRGS/1/2022/TK08/UNIMAS/02/10). The authors also thank Universiti Malaysia Sarawak (F02/PARTNERS/2107/2021) for supporting this project.

References

1. Dubey A.K. and Yadava V. Laser beam machining—a review. *International Journal of Machine Tools and Manufacture* **48**(6) (2008), 609-628.
2. Bakhtiyari A.N., Wang Z., Wang L., and Zheng H. A review on applications of artificial intelligence in modeling and optimization of laser beam machining. *Optics & Laser Technology* **135** (2021), 106721.
3. Gaitonde V., Karnik S., Rubio J.C., Correia A.E., Abrao A., and Davim J.P. Analysis of parametric influence on delamination in high-speed drilling of carbon fiber reinforced plastic composites. *Journal of materials processing technology* **203**(1-3) (2008), 431-438.
4. Tamrin K., Sheikh N., and Sapuan S. Laser drilling of composite material: A review. *Hole-Making and Drilling Technology for Composites* (2019), 89-100.

5. Oke S.R., Ogunwande G.S., Onifade M., Aikulola E., Adewale E.D., Olawale O.E., Ayodele B.E., Mwema F., Obiko J., and Bodunrin M.O. An overview of conventional and non-conventional techniques for machining of titanium alloys. *Manufacturing Review* **7** (2020), 34.
6. Ranjan C., Kalita H., Vardhan T.V., and Kumar K. Programming for Machining in Electrical Discharge Machine: A Non-Conventional Machining Technique, in *Machine Learning Applications in Non-Conventional Machining Processes*. IGI Global. 2021. p. 55-75.
7. Nagaraj Y., Jagannatha N., and Sathisha N. Hybrid Non Conventional Machining of Glass-A Review. *Applied Mechanics and Materials* **895** (2019), 8-14.
8. Kumar S. and Dvivedi A. On effect of tool rotation on performance of rotary tool micro-ultrasonic machining. *Materials and Manufacturing Processes* **34**(5) (2019), 475-486.
9. Sloyan K., Melkonyan H., Apostoleris H., Dahlem M.S., Chiesa M., and Al Ghaferi A. A review of focused ion beam applications in optical fibers. *Nanotechnology* **32**(47) (2021), 472004.
10. Farooq M.U., Anwar S., Kumar M.S., AlFaify A., Ali M.A., Kumar R., and Haber R. A Novel Flushing Mechanism to Minimize Roughness and Dimensional Errors during Wire Electric Discharge Machining of Complex Profiles on Inconel 718. *Materials* **15**(20) (2022), 7330.
11. El-Hofy M. and El-Hofy H. Laser beam machining of carbon fiber reinforced composites: a review. *The International Journal of Advanced Manufacturing Technology* **101**(9-12) (2019), 2965-2975.
12. Holmberg J., Berglund J., Wretland A., and Beno T. Evaluation of surface integrity after high energy machining with EDM, laser beam machining and abrasive water jet machining of alloy 718. *The International Journal of Advanced Manufacturing Technology* **100**(5) (2019), 1575-1591.
13. Steen W.M. and Mazumder J. *Laser material processing*. London: Springer-Verlag London Limited. 2010.
14. Parandoush P. and Hossain A. A review of modeling and simulation of laser beam machining. *International journal of machine tools and manufacture* **85** (2014), 135-145.
15. Riveiro A., Quintero F., Boutinguiza M., Del Val J., Comesaña R., Lusquiños F., and Pou J. Laser cutting: A review on the influence of assist gas. *Materials* **12**(1) (2019), 157.
16. Elsheikh A.H., Deng W., and Showaib E.A. Improving laser cutting quality of polymethylmethacrylate sheet: experimental investigation and optimization. *Journal of Materials Research and Technology* **9**(2) (2020), 1325-1339.
17. Kwon D.-J., Kim J.-H., Park S.-M., Kwon I.-J., DeVries K.L., and Park J.-M. Damage sensing, mechanical and interfacial properties of resins suitable for new CFRP rope for elevator applications. *Composites Part B: Engineering* **157** (2019), 259-265.
18. Al-Lami A., Hilmer P., and Sinapius M. Eco-efficiency assessment of manufacturing carbon fiber reinforced polymers (CFRP) in aerospace industry. *Aerospace Science and Technology* **79** (2018), 669-678.
19. Chouhan H., Singh D., Parmar V., Kalyanasundaram D., and Bhatnagar N. Laser machining of Kevlar fiber reinforced laminates—Effect of polyetherimide versus polypropylene matrix. *Composites Science and Technology* **134** (2016), 267-274.
20. Mohammed L., Ansari M.N., Pua G., Jawaid M., and Islam M.S. A review on natural fiber reinforced polymer composite and its applications. *International journal of polymer science* **2015** (2015).
21. Gholampour A. and Ozbakkaloglu T. A review of natural fiber composites: Properties, modification and processing techniques, characterization, applications. *Journal of Materials Science* **55**(3) (2020), 829-892.
22. SHAHARUDDIN S.S., JALIL M.H., and MOGHADASI K. Study of mechanical properties and characteristics of eco-fibres for sustainable children's clothing. *Journal of Metals, Materials and Minerals* **31**(2) (2021), 19-26.
23. Whitlow T., Jones E., and Przybyla C. In-situ damage monitoring of a SiC/SiC ceramic matrix composite using acoustic emission and digital image correlation. *Composite Structures* **158** (2016), 245-251.
24. Reddy P.S., Kesavan R., and Ramnath B.V. Investigation of mechanical properties of aluminium 6061-silicon carbide, boron carbide metal matrix composite. *Silicon* **10**(2) (2018), 495-502.
25. Prakash S. and Kumar S. Experimental investigations and analytical modeling of multi-pass CO2 laser processing on PMMA. *Precision Engineering* **49** (2017), 220-234.
26. Hong T.-F., Ju W.-J., Wu M.-C., Tai C.-H., Tsai C.-H., and Fu L.-M. Rapid prototyping of PMMA microfluidic chips utilizing a CO 2 laser. *Microfluidics and nanofluidics* **9**(6) (2010), 1125-1133.
27. Moghadasi K., Tamrin K.F., Sheikh N.A., and Jawaid M. A numerical failure analysis of laser micromachining in various thermoplastics. *The International Journal of Advanced Manufacturing Technology* **117**(1) (2021), 523-538.
28. Sharma A. and Yadava V. Experimental analysis of Nd-YAG laser cutting of sheet materials—A review. *Optics & Laser Technology* **98** (2018), 264-280.
29. Riveiro A., Quintero F., Lusquiños F., Del Val J., Comesaña R., Boutinguiza M., and Pou J. Experimental study on the CO2 laser cutting of carbon fiber reinforced plastic composite. *Composites Part A: Applied Science and Manufacturing* **43**(8) (2012), 1400-1409.
30. Yang L.J., Cheng X.L., Wang G.W., Xue Q.M., Ding Y., and Wang Y. *Experimental evaluation of cutting quality of carbon fibre reinforced polymer with pulsed laser*. in *Applied Mechanics and Materials*. 2017. Trans Tech Publ.
31. Moghadasi K. and Tamrin K.F. Experimental investigation and parameter optimization of low power CO2 laser cutting of a carbon/Kevlar fiber-reinforced hybrid composite. *Lasers in Engineering (Old City Publishing)* **45**(1-3) (2020), 85-108.

32. Leone C. and Genna S. Heat affected zone extension in pulsed Nd: YAG laser cutting of CFRP. *Composites Part B: Engineering* **140** (2018), 174-182.
33. Staehr R., Bluemel S., Jaeschke P., Suttman O., and Overmeyer L. Laser cutting of composites—Two approaches toward an industrial establishment. *Journal of Laser Applications* **28**(2) (2016), 022203.
34. Tamrin K., Moghadasi K., and Sheikh N. Experimental and numerical investigation on multi-pass laser cutting of natural fibre composite. *The International Journal of Advanced Manufacturing Technology* (2020), 1-22.
35. Herzog D., Schmidt-Lehr M., Oberlander M., Canisius M., Radek M., and Emmelmann C. Laser cutting of carbon fibre reinforced plastics of high thickness. *Materials & Design* **92** (2016), 742-749.
36. Leone C., Genna S., and Tagliaferri V. Fibre laser cutting of CFRP thin sheets by multi-passes scan technique. *Optics and Lasers in Engineering* **53** (2014), 43-50.
37. Rao S., Sethi A., Das A.K., Mandal N., Kiran P., Ghosh R., Dixit A., and Mandal A. Fiber laser cutting of CFRP composites and process optimization through response surface methodology. *Materials and Manufacturing Processes* **32**(14) (2017), 1612-1621.
38. Ghavidel A.K., Azdast T., Shabgard M.R., Navidfar A., and Shishavan S.M. Effect of carbon nanotubes on laser cutting of multi-walled carbon nanotubes/poly methyl methacrylate nanocomposites. *Optics & Laser Technology* **67** (2015), 119-124.
39. Nagesh S., Murthy H.N., Pal R., Dev S.S., and Krishna M. Investigation of the effect of nanofillers on the quality of CO₂ laser cutting of FRP nanocomposites. *The International Journal of Advanced Manufacturing Technology* **90**(5-8) (2017), 2047-2061.
40. Niino H., Kawaguchi Y., Sato T., Narazaki A., Kurosaki R., Muramatsu M., Harada Y., Anzai K., Wakabayashi K., and Nagashima T. Laser cutting of carbon fiber reinforced thermo-plastic (CFRTP) by IR laser irradiation. *Journal of Laser Micro Nanoengineering* **9**(2) (2014), 180.
41. Jaeschke P., Kern M., Stute U., Kracht D., and Haferkamp H. Laser processing of continuous carbon fibre reinforced polyphenylene sulphide organic sheets—Correlation of process parameters and reduction in static tensile strength properties. *Journal of Thermoplastic Composite Materials* **27**(3) (2014), 324-337.
42. Sapuan S., Tamrin K., Nukman Y., EL-SHEKEIL Y., HUSSIN M., and AZIZ S. Multiple-objective optimization in precision cutting of cocoa fiber reinforced composites.
43. Nattapat M., Marimuthu S., Kamara A., and Esfahani M.N. Laser surface modification of carbon fiber reinforced composites. *Materials and Manufacturing Processes* **30**(12) (2015), 1450-1456.
44. Negarestani R., Sundar M., Sheikh M., Mativenga P., Li L., Li Z., Chu P., Khin C., Zheng H., and Lim G. Numerical simulation of laser machining of carbon-fibre-reinforced composites. *Proceedings of the Institution of Mechanical Engineers, Part B: Journal of Engineering Manufacture* **224**(7) (2010), 1017-1027.
45. Salama A., Li L., Mativenga P., and Whitehead D. TEA CO₂ laser machining of CFRP composite. *Applied Physics A* **122**(5) (2016), 497.
46. Finger J., Weinand M., and Wortmann D. Ablation and cutting of carbon-fiber reinforced plastics using picosecond pulsed laser radiation with high average power. *Journal of Laser Applications* **25**(4) (2013), 042007.
47. Wu C.-W., Wu X.-Q., and Huang C.-G. Ablation behaviors of carbon reinforced polymer composites by laser of different operation modes. *Optics & Laser Technology* **73** (2015), 23-28.
48. Fürst A., Hipp D., Klotzbach A., Hauptmann J., Wetzig A., and Beyer E. Increased Cutting Efficiency due to Multi-Wavelength Remote-Laser-Ablation of Fiber-Reinforced Polymers. *Advanced Engineering Materials* **18**(3) (2016), 403-408.
49. Choudhury I. and Chuan P. Experimental evaluation of laser cut quality of glass fibre reinforced plastic composite. *Optics and Lasers in Engineering* **51**(10) (2013), 1125-1132.
50. Adalarasan R., Santhanakumar M., and Rajmohan M. Optimization of laser cutting parameters for Al6061/SiCp/Al₂O₃ composite using grey based response surface methodology (GRSM). *Measurement* **73** (2015), 596-606.
51. Tong Y., Bai S., Zhang H., and Ye Y. Laser ablation behavior and mechanism of C/SiC composite. *Ceramics International* **39**(6) (2013), 6813-6820.
52. Prakash S. and Kumar S. Profile and depth prediction in single-pass and two-pass CO₂ laser microchanneling processes. *Journal of Micromechanics and Microengineering* **25**(3) (2015), 035010.
53. Chen X. and Hu Z. An effective method for fabricating microchannels on the polycarbonate (PC) substrate with CO₂ laser. *The International Journal of Advanced Manufacturing Technology* **92**(1-4) (2017), 1365-1370.
54. Takahashi K., Tsukamoto M., Masuno S., Sato Y., Yoshida H., Tsubakimoto K., Fujita H., Miyayama N., Fujita M., and Ogata H. Influence of laser scanning conditions on CFRP processing with a pulsed fiber laser. *Journal of Materials Processing Technology* **222** (2015), 110-121.
55. Karimzad Ghavidel A., Navidfar A., Shabgard M., and Azdast T. Role of CO₂ laser cutting conditions on anisotropic properties of nanocomposite contain carbon nanotubes. *Journal of Laser Applications* **28**(3) (2016), 032006.
56. Yilbas B.S., Khan S., Raza K., Keles O., Ubeyli M., Demir T., and Karakas M.S. Laser cutting of 7050 Al alloy reinforced with Al₂O₃ and B₄C composites. *The International Journal of Advanced Manufacturing Technology* **50**(1-4) (2010), 185-193.
57. Affandi N.N., Tamrin K.F., Khan A.A., Moghadasi K., Sharip M.R.M., Mohamaddan S., and Hossain A. A Feasibility Study Of Low-Power Laser Trepanning Drilling Of Composite Using Modified DVD Writer. *International Journal of Integrated Engineering* **12**(3) (2020), 187-196.
58. Tamrin K., Nukman Y., Sheikh N., and Harizam M. Determination of optimum parameters using grey relational

- analysis for multi-performance characteristics in CO₂ laser joining of dissimilar materials. *Optics and Lasers in Engineering* **57** (2014), 40-47.
59. Bluemel S., Staehr R., Jaeschke P., Suttman O., and Overmeyer L. Correlation of internal and surface temperatures during laser cutting of epoxy-based carbon fibre reinforced plastics. *Journal of Reinforced Plastics and Composites* **34**(8) (2015), 662-671.
60. Xu H. and Hu J. Modeling of the material removal and heat affected zone formation in CFRP short pulsed laser processing. *Applied Mathematical Modelling* **46** (2017), 354-364.
61. Herzog D., Jaeschke P., Meier O., and Haferkamp H. Investigations on the thermal effect caused by laser cutting with respect to static strength of CFRP. *International journal of machine tools and manufacture* **48**(12-13) (2008), 1464-1473.
62. Takahashi K., Tsukamoto M., Masuno S., and Sato Y. Heat conduction analysis of laser CFRP processing with IR and UV laser light. *Composites Part A: Applied Science and Manufacturing* **84** (2016), 114-122.
63. Muramatsu M., Harada Y., Suzuki T., and Niino H. Infrared stress measurements of thermal damage to laser-processed carbon fiber reinforced plastics. *Composites Part A: Applied Science and Manufacturing* **68** (2015), 242-250.
64. Tamrin K.F., Zakariyah S., Hossain K., and Sheikh N.A. Experiment and prediction of ablation depth in excimer laser micromachining of optical polymer waveguides. *Advances in Materials Science and Engineering* **2018** (2018), 9.
65. Herzog D., Schmidt-Lehr M., Canisius M., Oberlander M., Tasche J.-P., and Emmelmann C. Laser cutting of carbon fiber reinforced plastic using a 30 kW fiber laser. *Journal of Laser Applications* **27**(S2) (2015), S28001.
66. Tamrin K.F., Khalid N.A., and Rigit A.R.H. Fabrication of Flexible Microfluidic Strain Sensor by Laser Micromachining for Hand Motion Tracking. *Laser* **20**(25) (2020), 30.
67. Shyha I. An investigation into CO₂ laser trimming of CFRP and GFRP composites. *Procedia Engineering* **63** (2013), 931-937.
68. Patel P., Sheth S., and Patel T. Experimental analysis and ANN modelling of HAZ in laser cutting of glass fibre reinforced plastic composites. *Procedia Technology* **23** (2016), 406-413.
69. Fatimah S., Ishak M., and Aqida S. *CO₂ laser cutting of glass fiber reinforce polymer composite*. in *IOP conference series: materials science and engineering*. 2012. IOP Publishing.
70. Tamrin K.F., Nukman Y., Choudhury I., and Shirley S. Multiple-objective optimization in precision laser cutting of different thermoplastics. *Optics and Lasers in Engineering* **67** (2015), 57-65.
71. Moghadasi K. and Tamrin K. Multi-pass laser cutting of carbon/Kevlar hybrid composite: Prediction of thermal stress, heat-affected zone, and kerf width by thermo-mechanical modeling. *Proceedings of the Institution of Mechanical Engineers, Part L: Journal of Materials: Design and Applications* **234**(9) (2020), 1228-1241.
72. Tamrin K.F., Moghadasi K., Jalil M.H., Sheikh N.A., and Mohamaddan S. Laser discoloration in acrylic painting of visual art: Experiment and modeling. *Materials* **14**(8) (2021), 2009.
73. Moghadasi K., *Experimental and Numerical Investigation of CO₂ Laser Cutting of Carbon/Kevlar Hybrid Composite*, in *Mechanical and Manufacturing Engineering*. 2020, Universiti Malaysia Sarawak (UNIMAS): Malaysia. p. 146.
74. Yilbas B. and Akhtar S. Laser cutting of Kevlar laminates and thermal stress formed at cutting sections. *Optics and Lasers in Engineering* **50**(2) (2012), 204-209.
75. Yilbas B., Akhtar S., and Karatas C. Laser circular cutting of Kevlar sheets: Analysis of thermal stress field and assessment of cutting geometry. *Optics & Laser Technology* **96** (2017), 180-189.
76. Moradi M., Moghadam M.K., Shamsborhan M., Beiranvand Z.M., Rasouli A., Vahdati M., Bakhtiari A., and Bodaghi M. Simulation, statistical modeling, and optimization of CO₂ laser cutting process of polycarbonate sheets. *Optik* (2020), 164932.
77. Liu Y.-C., Wu C.-W., Huang Y.-H., Song H.-W., and Huang C.-G. Interlaminar damage of carbon fiber reinforced polymer composite laminate under continuous wave laser irradiation. *Optics and Lasers in Engineering* **88** (2017), 91-101.
78. Sun D., Han F., and Ying W. Numerical simulation of water jet-guided laser cutting of carbon fiber-reinforced plastics. *Proceedings of the Institution of Mechanical Engineers, Part B: Journal of Engineering Manufacture* (2018), 0954405418809776.
79. Long L., Huang Y., and Zhang J. Experimental investigation and numerical simulation on continuous wave laser ablation of multilayer carbon fiber composite. *Proceedings of the Institution of Mechanical Engineers, Part L: Journal of Materials: Design and Applications* **231**(8) (2017), 674-682.
80. Ohkubo T., Sato Y., Matsunaga E.-i., and Tsukamoto M. Three-dimensional numerical simulation during laser processing of CFRP. *Applied Surface Science* **417** (2017), 104-107.

